

**Figure 1.** Structure of the title compound (**1**) showing the atom numbering scheme. For clarity, H atoms have been omitted and only one orientation of the ester groups is shown. Selected interatomic distances: Cu-S(1), 2.230 (5); Cu-S(2), 2.262 (4); Cu-N(1), 2.002 (11); Cu-N(2), 2.059 (13); S(1)···S(2), 3.406 (6) Å. Selected bond angles: S(1)-Cu-S(2), 98.6 (2)°; S(1)-Cu-N(1), 89.7 (4)°; S(1)-Cu-N(2), 165.1 (3)°; S(2)-Cu-N(1), 162.6 (4)°; S(2)-Cu-N(2), 88.4 (4)°; Cu-S(1)-C(1), 97.0 (5)°; Cu-S(2)-C(6), 96.8 (6)°; N(1)-Cu-N(2), 87.2 (5)°.

present.<sup>17</sup> The structure of this neutral monomer is shown in Figure 1. The Cu-S(1)-S(2)/Cu-N(1)-N(2) angle (21.0°) defines the small pseudotetrahedral twist of the approximately planar cis CuN<sub>2</sub>S<sub>2</sub> unit; the Ni(II) analogue is structurally similar.<sup>19</sup> Observed Cu-S distances are longer than that in plastocyanin (X-ray, 2.13 Å; EXAFS, 2.08–2.10 Å),<sup>20</sup> shorter than those in Cu(tet *b*)-2-mercaptobenzoate<sup>15</sup> (2.359 (4) Å) (**3**) and the mercaptopropionate analogue **2**<sup>1</sup> (2.314 (2) Å), and agree well with the average Cu-S distance determined by EXAFS (2.27 (2) Å) for cytochrome *c* oxidase.<sup>10</sup> The Cu-S-C bond angles are smaller than those reported for **3**<sup>15</sup> (108.4 (4)°) plastocyanin<sup>21</sup> (107°), and **2**<sup>1</sup> (115.9(2)°). The intramolecular S(1)···S(2) distance is shorter than the van der Waals contact of 3.7 Å. Shorter S···S contacts (≈2.8 Å) are present in Mo(VI) complexes with O<sub>2</sub>N<sub>2</sub>S<sub>2</sub> donor sets.<sup>22</sup> The bulky ester groups are equatorially oriented on the λ conformation NS chelate rings.<sup>23</sup> Stable analogues of **1** can be prepared from ester-free, linear tetradentate amino thiol ligands.<sup>24</sup>

(17) Crystallography: CuS<sub>2</sub>O<sub>4</sub>N<sub>2</sub>C<sub>10</sub>H<sub>18</sub>, *P*1, *a* = 5.508 (1) Å, *b* = 12.402 (2) Å, *c* = 5.500 (6) Å, α = 102.23 (2)°, β = 90.14 (2)°, γ = 77.75 (2)°, *V* = 358.4 (6) Å<sup>3</sup>, *Z* = 1; *d*<sub>obsd</sub> = 1.64 (1), *d*<sub>calcd</sub> = 1.66 g/cm<sup>3</sup>. The structure was solved by using 884 unique reflections (*I* > 3σ(*I*)) collected with Mo Kα radiation (λ = 0.71073 Å) to 2θ = 50° using an Enraf-Nonius CAD-4 diffractometer. All atoms were located on completely occupied sites except for certain ester group atoms (O(1)–O(4), C(9), C(10)), which were located on half-occupied sites. Refinement with all atoms anisotropic except those of the ester groups yielded *R*<sub>F</sub> = 0.057, *R*<sub>wF</sub> = 0.065, and GOF = 1.80. The crystal is multiply twinned with [101] as the twin diad axis which interchanges *a* and *c* and converts *b* to *-b*. Except for the disordered atoms, it generates a pseudo-two-fold axis in the molecule with equivalent atoms at *x,y,z* and *z,-y,x*. The structure factors reflect this equivalence: |*F*<sub>hkl</sub>| = |*F*<sub>h̄k̄l̄</sub>|. Refinement of the multipliers of the disordered C and O atoms showed that these sites were indeed half-occupied and that the twin volumes were equal. Thus, it is not possible to refine the twins individually.<sup>18</sup> Finally, the twinning causes unusual orientations of some thermal ellipsoids and larger than expected esd's of coordinates and derived parameters for a structure at this level of refinement.

(18) Sabelli, C.; Tangocci, P.; Zanazzi, P. F. *Acta Crystallogr., Sect B* 1969, B25, 2231.

(19) Both the Ni(II) analogue of **1** and H<sub>3</sub>NCH<sub>2</sub>CH<sub>2</sub>NH<sub>3</sub>[Ni(SCH<sub>2</sub>CH(CO<sub>2</sub>)NHCH<sub>2</sub>-)]<sub>2</sub>, the diacidate form of the N<sub>2</sub>S<sub>2</sub> ligand, have been characterized: Bharadwaj, P. K.; Potenza, J. A.; Schugar, H. J., manuscript in preparation.

(20) Scott, R. A.; Hahn, J. E.; Doniach, S.; Freeman, H. C.; Hodgson, K. O. *J. Am. Chem. Soc.* 1982, 104, 5364 and references cited therein.

(21) Penfield, K. W.; Gay, R. R.; Himmelwright, R. S.; Eickman, N. C.; Norris, V. A.; Freeman, H. C.; Solomon, E. I. *J. Am. Chem. Soc.* 1981, 103, 4382.

(22) Berg, J. M.; Spira, D. J.; Hodgson, K. O.; Bruce, A. E.; Miller, K. F.; Corbin, J. L.; Stiefel, E. I. *Inorg. Chem.* 1984, 23, 3412 and references cited therein.

(23) Buchanan, I.; Minelli, M.; Ashby, M. T.; King, T. J.; Enemark, J. H.; Garner, C. D. *Inorg. Chem.* 1984, 23, 495.

(24) Bharadwaj, P. K.; Firkar, R.; Potenza, J. A.; Schugar, H. J., unpublished results.

The magnetic moment (1.70 (4) μ<sub>B</sub>)<sup>25</sup> and spectroscopic features of **1** are those of Cu(II). The isotropic EPR parameters (DMF, 298 K) are *g*<sub>iso</sub> = 2.066 and *A*<sub>iso</sub><sup>Cu</sup> = 88 × 10<sup>-4</sup> cm<sup>-1</sup>; at 80 K (in DMF or the Ni(II) analogue), the spectra are those of a tetragonal Cu(II) species with *g*<sub>||</sub> = 2.126, *g*<sub>⊥</sub> = 2.039, *A*<sub>||</sub><sup>Cu</sup> = 182 × 10<sup>-4</sup> cm<sup>-1</sup>, and *A*<sub>⊥</sub><sup>Cu</sup> = 49 × 10<sup>-4</sup> cm<sup>-1</sup>. An absorption at 545 nm (ε ≈ 1000) is assigned as a LF band, possibly enhanced by "intensity stealing" from the nearby LMCT bands.<sup>26</sup> The near-UV bands at ≈400 nm (sh, ε > 1000) and 345 nm (ε ≈ 5800) are those of thiolate → Cu(II) LMCT for complexes having typical (i.e., nontetrahedral) geometries.<sup>1,15,27</sup> The EPR parameters and absorption maxima are remarkably similar to those of the unstable bis Cu(II) complexes of L-cysteine and other NS donor ligands.<sup>28-30</sup> Finally, the presence of two cysteine ligands does not in itself generate either the peculiar EPR or intense 600-nm absorption of the Cu<sub>A</sub> protein site.<sup>3</sup> The additional effects of imidazole ligation and tetrahedral distortion are being explored.

**Acknowledgment.** This research was supported by the National Science Foundation (Grant CHE-8417548), the David and Joanna Busch Foundation, and the National Institutes of Health (Instrumentation Grant 1510 RRO 1486 O1A1).

**Supplementary Material Available:** Tables of atomic coordinates, thermal parameters, bond distances and angles, and observed and calculated structure factors (13 pages). Ordering information is given on any current masthead page.

(25) The magnetic moment at 298 K includes a diamagnetic correction of -181 × 10<sup>-6</sup> cgs from Pascal's constants.

(26) Miskowski, V. M.; Thich, J. A.; Solomon, R.; Schugar, H. J. *J. Am. Chem. Soc.* 1976, 98, 8344.

(27) Anderson, O. P.; Perkins, C. M.; Brito, K. K. *Inorg. Chem.* 1983, 22, 1267.

(28) Cavallini, D.; DeMarco, C.; Dupre, S.; Rotilio, G. *Arch. Biochem. Biophys.* 1969, 130, 354.

(29) Hanaki, A.; Kamide, H. *Chem. Pharm. Bull.* 1975, 23, 1671.

(30) Davis, F. J.; Gilbert, B. C.; Norman, R. O. C. *J. Chem. Soc., Perkins Trans. 2* 1983, 1763 and references therein.

## Models of Heme *d*<sub>1</sub>. Structure and Redox Chemistry of Dioxoisobacteriochlorins

C. K. Chang\*

Department of Chemistry, Michigan State University  
East Lansing, Michigan 48824

K. M. Barkigia,<sup>1</sup> L. K. Hanson, and J. Fajer\*

Department of Applied Science  
Brookhaven National Laboratory  
Upton, New York 11973

Received November 22, 1985

Unlike the ubiquitous iron porphyrin containing cytochromes found in animals and plants, *d*-type cytochromes present in many microbial nitrite reductases–cytochrome oxidases contain a green heme prosthetic group whose structure has been assumed for the last 2 decades to be a chlorin (dihydroporphyrin).<sup>2</sup> On the basis of spectroscopic data collected by Timkovich et al.,<sup>3</sup> one of us (C.K.C.) has recently proposed that heme *d*<sub>1</sub> isolated from *Pseudomonas aeruginosa* and *Parracoccus denitrificans* is not a chlorin but a dioxoisobacteriochlorin.<sup>4</sup> Crucial to this as-

(1) Address inquiries regarding the crystallographic data to this author.

(2) Yamanaka, T.; Okunuki, K. *Biochim. Biophys. Acta* 1963, 67, 407-416.

(3) Timkovich, R.; Cork, M. S.; Taylor, P. V. *J. Biol. Chem.* 1984, 259, 1577-1585.

(4) Chang, C. K. *J. Biol. Chem.* 1985, 260, 9520-9522.

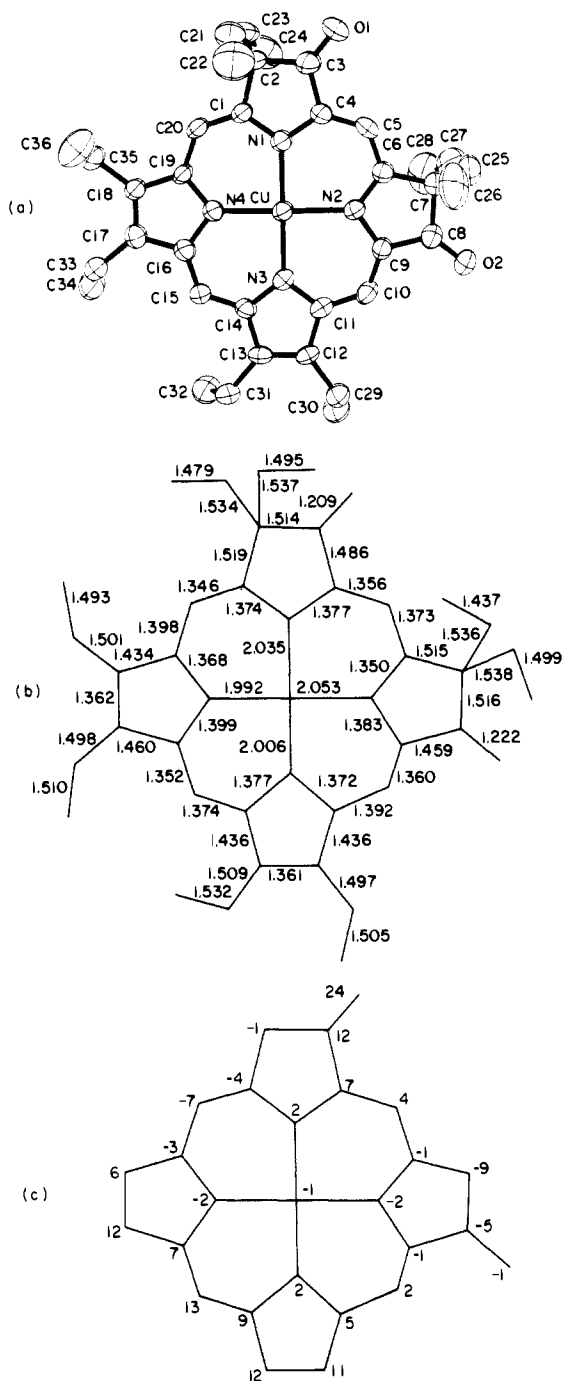


**Figure 1.** (a) Molecular structure and atom names of **2**. Ellipsoids are drawn to enclose 50% probability. Hydrogen atoms have been omitted for clarity. (b) Bond distances (Å). The esd's are 0.005 Å for the Cu-N bond, 0.008 Å for the skeleton distances, and 0.010 Å for the side chains. (c) Deviations ( $\text{Å} \times 10^2$ ) from the plane of the four nitrogens.

segment is a model compound, 3,8-dioxo-2,2',7,7',12,13,17,18-octaethylporphyrin (**1**, dioxo iBC),<sup>5</sup> which exhibits many diagnostic NMR and absorption spectral features also possessed by the natural  $d_1$  pigment.<sup>6</sup> As part of an investigation to establish the validity of this proposal, we report here physicochemical properties of several oxoporphyrin derivatives,<sup>7</sup> a family of compounds that

(5) Abbreviations: P, porphyrin; C, chlorin, a porphyrin in which one  $\beta$ - $\beta$  pyrrole bond is saturated; iBC, isobacteriochlorin, and BC, bacteriochlorin, porphyrins in which two  $\beta$ - $\beta$  pyrrole bonds are saturated on adjacent and opposite rings, respectively; OEP, 2,3,7,8,12,13,17,18-octaethylporphyrin; Oxochlorin, 3-oxo-2,2',7,8,12,13,17,18-octaethylporphyrin; dioxo iBC, 3,8-dioxo-2,2',7,7',12,13,17,18-octaethylporphyrin; dioxo BC, 3,13-dioxo-2,2',7,8,12,12',17,18-octaethylporphyrin.

(6) Chang, C. K.; Timkovich, R., unpublished results.

**Table I.** Redox Potentials of Porphyrins and Oxoporphyrins (vs. SCE)<sup>a</sup>

compound	ring/ring <sup>+</sup>	Fe(III)/Fe(II)	ring/ring <sup>-</sup>
porphyrin (OEP) <sup>5</sup>			
H <sub>2</sub>	0.83		-1.46
Cu	0.73		-1.46
FeCl	0.9	-0.5 <sup>b</sup>	
Fe(MeIm) <sub>2</sub> <sup>c</sup>		-0.37	
Fe(MeIm)CO		0.38 <sup>d</sup>	
oxochlorin <sup>5</sup>			
H <sub>2</sub>	0.84		-1.36
Cu	0.68		-1.37
FeCl	0.95	-0.34 <sup>b</sup>	
Fe(MeIm) <sub>2</sub> <sup>c</sup>		-0.19	
Fe(MeIm)CO		0.41 <sup>d</sup>	
dioxoisobacteriochlorin <sup>5</sup>			
H <sub>2</sub>	0.82		-1.29
Cu	0.67		-1.27
FeCl	0.84	-0.24 <sup>b</sup>	
Fe(MeIm) <sub>2</sub> <sup>c</sup>		0.06	
Fe(MeIm)CO		0.53 <sup>d</sup>	
dioxobacteriochlorin <sup>5</sup>			
H <sub>2</sub>	0.82		-1.19

<sup>a</sup>  $E_{1/2}$  obtained by cyclic voltammetry at a Pt electrode in CH<sub>2</sub>Cl<sub>2</sub> containing 0.1 M tetrabutylammonium perchlorate. <sup>b</sup> Quasi-reversible. <sup>c</sup> In 2 M *N*-methylimidazole. <sup>d</sup> Irreversible loss of CO.

has received little attention, hitherto.

The results of an X-ray study of the Cu(II) complex of **1** establish the molecular structure of the dioxoisobacteriochlorin class, and redox data for iron and other dioxoisobacteriochlorins and oxochlorins reveal that the introduction of oxo and dioxo functions significantly alters the redox properties of chlorins (C) and isobacteriochlorins (iBC) and renders the oxo derivatives more akin to porphyrins (P). The substitution effects on these redox properties agree with the migration of the HOMOs and LUMOs calculated by charge iterative extended Hückel methods.

The Cu(II) complex **2** of the dioxo iBC (**1**) crystallizes from dichloroethane/ethanol mixtures in the space group  $P2_1/c$  with  $Z = 4$ . The molecular structure of **2**, atom names, bond distances, and deviations from planarity<sup>10</sup> are presented in Figure 1. The long and short  $\beta$ - $\beta$  bonds in the saturated and unsaturated pyrroles are similar to those observed in other hydrophyrins, i.e., C's, iBC's, and bacteriochlorins (BC's). The inductive effects of the oxo groups are reflected in the asymmetries of rings I and II. The  $\alpha$ - $\beta$  bonds bearing the oxygens (C3-C4 and C8-C9) are significantly shorter (1.486 (8) and 1.459 (8) Å) than the opposite  $\alpha$ - $\beta$  bonds of the pyrrolidines: C1-C2 = 1.519 (7) and C6-C7 = 1.515 (8) Å. (A similar effect is found in the bacteriochlorin 3,13-dimethylene-2,2',7,8,12,12',17,18-octaethylporphyrin<sup>11</sup> where C3-C4 = 1.479 and C1-C2 = 1.532 Å.) As observed in other hydrophyrins,<sup>11,12</sup> the metal-to-nitrogen distances in the dioxo compound are longer to the saturated rings than to the pyrroles: Cu-N1 = 2.035 (4) and Cu-N2 = 2.053 (5), vs. Cu-N3 = 2.006 (5) and Cu-N4 = 1.992 (5) Å. Cu-N1 and Cu-N2 are com-

(7) The oxo derivatives of octaethylporphyrin were prepared and purified as previously described.<sup>8,9</sup> Metals were inserted by standard techniques using copper(II) acetate or iron(II) sulfate.

(8) Inhoffen, H. H.; Nolte, W. *Liebigs Ann. Chem.* **1969**, 725, 167-176.

(9) Chang, C. K. *Biochemistry* **1980**, 19, 1971-1976.

(10) Compound **2**, (3,8-dioxo-2,2',7,7',12,13,17,18-octaethylporphyrinato)-copper(II), crystallized as CuN<sub>4</sub>C<sub>36</sub>O<sub>2</sub>H<sub>44</sub>·1/2C<sub>2</sub>Cl<sub>2</sub>H<sub>4</sub> in the monoclinic space group  $P2_1/c$  in a unit cell of dimensions  $a = 13.571$  (4) Å,  $b = 10.781$  (3) Å,  $c = 24.086$  (10) Å,  $\beta = 92.50$  (3)°,  $V = 3520.6$  Å<sup>3</sup>,  $Z = 4$ . A total of 11 109 reflections ( $4^\circ \leq 2\theta \leq 45^\circ$ ,  $h, \pm k, \pm l$ ) were measured on a CAD-4 diffractometer using Mo K $\alpha$  radiation and averaged to yield 4901 unique data. The structure was solved with MULTAN 78 and refined in two blocks by using full-matrix least squares against the 2966 data having  $F_o \geq 3\sigma F_o$  to final values of  $R_F = 0.062$  and  $R_w F = 0.059$ . Hydrogen atoms were included in the model as fixed atom contributions.

(11) Barkigia, K. M.; Fajer, J.; Chang, C. K.; Young, R. *J. Am. Chem. Soc.* **1984**, 106, 6457-6459 and references therein.

(12) (a) Kratky, C.; Waditschatka, R.; Angst, C.; Johansen, J. E.; Plaquevent, J. C.; Schreiber, J.; Eschenmoser, A. *Helv. Chim. Acta* **1985**, 68, 1312-1337 and references therein. (b) Strauss, S. H.; Silver, M. E.; Ibers, J. A. *J. Am. Chem. Soc.* **1983**, 105, 4108-4109.

parable to the analogous distances found in a Cu(II) hexahydroporphyrin<sup>12a</sup> whereas Cu-N3 and Cu-N4 are typical of Cu-N distances reported in several Cu porphyrins.<sup>13</sup>

The macrocycle itself is nearly planar (see Figure 1) with the largest displacements from the plane of the four nitrogens of 0.12 Å at C3, C13, and C17, of 0.13 Å at C15, and of 0.24 Å at O1. The oxygens lie 0.08 and 0.07 Å out of the planes of rings I and II, respectively. The molecule is slightly buckled: angles between the planes of the rings are 5.6° (I and II), 5.7° (I and III), 1.9° (II and III), 7.4° (I and IV), 2.3° (II and IV), and 1.9° (III and IV). Overall, these deviations from planarity are small compared to those of some free base<sup>14</sup> and nickel iBC's.<sup>12a,15</sup> The "planarity" is consonant with that of some other Cu porphyrins<sup>13</sup> and with the additional rigidity imposed by the exocyclic double bonds to the oxygens. Some of the deviations from planarity may also be due to the packing: the molecules of **2** form dimers in which rings III of neighbors overlap with a mean plane separation of 3.77 Å and a Cu-Cu distance of 6.12 Å. (An illustration of the overlap is included in the supplementary material.)

The redox chemistry of oxochlorins and dioxo iBC's and BC's has been examined by cyclic voltammetry. The results are listed in Table I. Surprisingly, the oxo compounds exhibit ring oxidation potentials very similar to those of the parent porphyrin, in sharp contrast to those of C's, iBC's, and BC's, which are significantly easier to oxidize than the porphyrin (by as much as 0.6 V<sup>16,17</sup>). An immediate consequence of this invariance is that the Fe<sup>II</sup>CO complex of **1** oxidizes to Fe(III) with concomitant loss of CO as opposed to Fe<sup>II</sup>(CO)iBC, which yields a stable Fe<sup>II</sup>(CO)iBC<sup>+</sup>  $\pi$  cation on oxidation.<sup>16</sup> Again, in contrast to the behavior of iBC derivatives, which are harder to reduce than P's by  $\sim 0.3$  V,<sup>16,17</sup> the dioxo iBC's are easier to reduce by  $\sim 0.2$  V for a net change of  $\sim 0.5$  V in reduction potential upon introduction of the dioxo functions onto the iBC skeleton. Note that the Fe(II)/Fe(III) couples also shift so that metal-centered reductions become easier.

Extended Hückel MO calculations help rationalize the observed redox trends and indicate that the HOMOs in P's, oxo C's, and dioxo iBC's and BC's fall within a narrow energy range, unlike those in C's, BC's, and iBC's. For example, the calculated energies for the HOMOs of model Zn complexes are as follows: ZnP, -11.159; Zn oxo C, -11.189; Zn dioxo iBC, -10.953; Zn dioxo BC, -10.935; ZnC,<sup>16</sup> -10.823; ZniBC,<sup>16</sup> -10.338; ZnBC,<sup>16</sup> -10.279 eV. The more negative orbital energies correspond to harder to oxidize molecules. For reduction potentials, the more negative LUMOs will translate into easier to reduce molecules. LUMO energies are as follows: ZnP, -9.195; Zn oxo C, -9.394; Zn dioxo iBC, -9.276; Zn dioxo BC, -9.547; ZniBC,<sup>16</sup> -8.752 eV. The calculated net charges on the metal also increase with addition of oxo groups, which should therefore result in the metal being harder to oxidize, as observed. The experimental redox trends are thus reasonably well predicted by the MO calculations.

The consequences of these properties in the chemistry of oxo compounds with substrates such as nitrites and nitrosyls, and their possible biological roles in dissimilatory nitrite reductases, are under investigation.

**Acknowledgment.** This work was supported by the Division of Chemical Sciences, U.S. Department of Energy, under Contract DE-AC02-76CH000016 at Brookhaven National Laboratory and by National Institutes of Health Grant GM 34468 at Michigan State University.

(13) Moustakali, I.; Tulinsky, A. *J. Am. Chem. Soc.* **1973**, *95*, 6811-6815. Collman, J. P.; Chong, A. O.; Jameson, G. B.; Oakley, R. T.; Rose, E.; Schmittou, E. R.; Ibers, J. A. *Ibid.* **1981**, *103*, 516-533. Hatada, M. H.; Tulinsky, A.; Chang, C. K. *Ibid.* **1980**, *102*, 7115-7116. Sheldrick, W. S. *Acta Crystallogr., Sect. B* **1978**, *B34*, 663-665.

(14) Barkigia, K. M.; Fajer, J.; Chang, C. K.; Williams, G. J. B. *J. Am. Chem. Soc.* **1982**, *104*, 315-317.

(15) Suh, M. P.; Swepston, P. N.; Ibers, J. A. *J. Am. Chem. Soc.* **1984**, *106*, 5164-5171.

(16) Chang, C. K.; Hanson, L. K.; Richardson, P. R.; Young, R.; Fajer, J. *Proc. Natl. Acad. Sci. U.S.A.* **1981**, *78*, 2652-2656.

(17) Stolzenberg, A. M.; Strauss, S. H.; Holm, R. H. *J. Am. Chem. Soc.* **1981**, *103*, 4763-4775. Chang, C. K.; Fajer, J. *Ibid.* **1980**, *102*, 848-851.

**Supplementary Material Available:** Positional and thermal parameters for the non-hydrogen atoms of **2** and an illustration of the overlap of neighboring molecules (3 pages). Ordering information is given on any current masthead page.

## Magnetic Alignment Effects in the 500-MHz <sup>1</sup>H NMR Spectrum of *o*-Dichlorobenzene in Acetone-*d*<sub>6</sub>

Frank A. L. Anet

Department of Chemistry and Biochemistry  
University of California  
Los Angeles, California 90024

Received October 18, 1985

High magnetic fields (e.g., 10 T) can induce an observable partial alignment of diamagnetic molecules in ordinary isotropic solutions.<sup>1</sup> Because this effect is extremely small, detection by <sup>1</sup>H NMR has only been realized in polycyclic molecules that have large anisotropic magnetic susceptibilities.<sup>2</sup> The NMR spectra of such molecules have a field dependence which allows direct coupling constants (*D*'s) to be obtained.<sup>3</sup> In deuterated molecules, <sup>2</sup>H NMR at a single magnetic field can provide information on the alignment of even simple aromatic molecules,<sup>2</sup> but this method has some limitations.<sup>4</sup>

Strongly resolution enhanced <sup>1</sup>H NMR spectra at a single high magnetic field of *symmetrical* systems are now shown to give information on extremely small direct coupling constants (down to a few millihertz), provided that frequencies can be measured to a fraction of 1 mHz.<sup>5</sup> The presence of residual second-order *J* splittings is essential for observing very small *D*'s in these cases. The simplest example of a second-order splitting occurs in the three-spin A<sub>2</sub>X-A<sub>2</sub>B system, which in the first-order limit (i.e., a large chemical shift difference) shows a 1:1 doublet (separation = *J*<sub>AX</sub>) for the A<sub>2</sub> nuclei. When the A-X chemical shift difference is no longer very large, the system becomes strictly of the A<sub>2</sub>B type, and both A<sub>2</sub> lines split into narrowly spaced doublets. These second-order splittings are modified when *D*<sub>AA</sub> is nonzero: one splitting increases whereas the other decreases.<sup>6</sup> The values and the relative signs of *D*<sub>AA</sub> and *J*<sub>AB</sub> can be determined, even if *D*<sub>AA</sub> is less than the line width. Similar effects are predicted for other *symmetrical* spin systems, such as A<sub>3</sub>B, A<sub>3</sub>B<sub>2</sub>, and AA'BB'. In all cases, only *D*'s between *isochronous nuclei* are easily measured at a single high magnetic field.

(1) For a recent review on molecular alignment in *normal liquids*, see: van Zijl, P. C. M.; Ruessink, B. H.; Bulthuis, J.; MacLean, C. *Acc. Chem. Res.* **1984**, *17*, 172-180.

(2) Gayathri, C.; Bothner-By, A. A.; van Zijl, P. C. M.; MacLean, C. *Chem. Phys. Lett.* **1982**, *87*, 192-196. The molecules studied were coronene and a porphyrin derivative. A referee has pointed out that some simpler molecules, namely, berberine and adenine, have also been successfully studied: Gayathri, C. Ph. D. Thesis, Carnegie-Mellon University, Pittsburgh, PA.

(3) The definition of *D* in this paper is the same as that used by MacLean and co-workers.<sup>1,2</sup> These *D*'s must be divided by two when used with computer programs such as MIMER (Manschen, O. H.; Jacobson, J. P.; Schaumberg, K. QCPE, University of Indiana, Bloomington, IN, Program 394). The value of *D*<sub>HH</sub> depends on the square of the magnetic field, the inverse cube of the H-H distance, and the averaged orientation of the H-H vector with respect to the magnetic field.

(4) (a) Alignment effects on <sup>2</sup>H spectra are larger than those on <sup>1</sup>H spectra because the quadrupole coupling constant in a C-D bond is up to an order of magnitude larger than the dipole-dipole interaction for a typical proton pair.<sup>1,2</sup> However, relaxation effects, which lead to line broadening, are proportional to the square of the (unaveraged) interactions, and consequently <sup>1</sup>H spectra are inherently more sensitive to alignment effects than are <sup>2</sup>H spectra.

(5) For other examples of ultrahigh resolution and/or ultrahigh accuracy in NMR spectra, see: Allerhand, A.; Addleman, R. E.; Osman, D. *J. Am. Chem. Soc.* **1985**, *107*, 5809-5810. Ellison, S. L. R.; Fellows, M. S.; Robinson, M. J. T.; Widger, M. J. *J. Chem. Soc., Chem. Commun.* **1984**, 1069.

(6) Diehl, P.; Khetrapal, C. L. In "NMR, Basic Principles and Progress"; Diehl, P., Fluck, E., Kosfeld, R., Eds.; Springer: Berlin, 1969; Vol. 1, pp 1-95. An expansion of the expressions for the transition frequencies in the near A<sub>2</sub>X limit with the *D*'s being small gives the second-order splittings as  $|J_{AB}^2/2\Delta\nu_{AB} \pm (3/2)D_{AA}|$ .